ChemElectroChem

Research Article
doi.org/10.1002/celc.202400158

Chemistry Europe
European Chemical Societies Publishing

www.chemelectrochem.org

Probing Carbon Materials Towards the Vanadium(IV)/(V) Reaction by Scanning Electrochemical Microscopy

Matthias Steimecke,*[a] Jens Carthäuser,[a] Lena Fiedler,[b] Emil Dieterich,[a] and Michael Bron[a]

A method is presented to quantitatively analyze the reduction of vanadium(V) to vanadium(IV) over two flat carbon substrates (glassy carbon and graphite foil) using the feedback mode of scanning electrochemical microscopy. A pulse profile is validated and applied during approach curve experiments of a 10 μm Pt microelectrode. By fitting the approach curve data, electron transfer constants are calculated for various potentials and k_0 is extracted from the corresponding Tafel plot. Furthermore, surface functional groups were introduced to the carbon substrates by acid treatment; however, kinetic parameters of the sluggish reduction reaction were only influenced to a minor extent. Finally, the same approach, combined with *in situ*-Raman microscopy, is applied to a single graphene layer using a 2.7 μm Pt microelectrode. In this case, increased activity for both, the vanadium(V) reduction and vanadium(IV) oxidation reaction, was found close to the graphene edge sites by means of electrochemical microscopy for the first time.

Introduction

The all-vanadium redox flow battery (VRFB) is a powerful state-of-the-art technology for the storage of fluctuating energy from wind and solar sources and has received growing attention over the last decade. Beside many other advantages, which are in common for all flow batteries, the all-vanadium type is the only one with a single element on both sides of the redox cell that can be converted to any involved oxidation state. Consequently, cross contamination only leads to capacity loss that can be fully regenerated afterwards. Since its first description by Skyllas-Kazacos and co-workers[1], a large body of research work has been carried out to understand the electrode processes in more detail, in particular for the positive half-cell reaction, where VO^{2+} ions are oxidized to VO_2^+ in case of charging and reduced in case of discharging. Carbon materials are widely accepted as the most suitable electrode material in terms of pricing and availability,[2] whereas the modification with bismuth may be useful for the negative half-cell of the battery to avoid hydrogen evolution (HER).[3] However, there is an ongoing debate in the literature on the nature of the active sites for the redox conversions as well as the mechanism at such carbon electrodes as well as the influence of pretreatment.[4] At the positive side, oxygen-containing groups at the carbon electrode surface were initially thought to play a key role.[5] In consequence, numerous methods of surface functionalization were suggested to introduce oxygen-containing groups into carbon electrodes; however, no consistent results concerning the influence towards the positive redox reaction were found.[6] The main reason for this is the necessity of separating catalytic effects from surface area changes by the treatment of the porous carbon materials, such as carbon felt, fleece or paper that are commonly used as electrodes in the VRFB. Therefore, more sophisticated methods were suggested such as applying chrono amperometry and electrochemical impedance spectroscopy to separate those effects.[7] Nevertheless, there is a consensus that a small quantity of oxygen-containing surface groups are useful for an improved wetting of the otherwise hydrophobic carbon surface.[8],[9] In contrast, flat carbon electrodes suffer from slow kinetics and a low symmetry of the reaction as observed for GC[10] and graphite[11] electrodes which may as well originate from adsorbed reaction intermediates. Different contributions from basal and edge carbon sites are discussed as well.[12] Scanning electrochemical microscopy (SECM) is a well-established technique, which allows the localized probing of electrochemical reactions which appear in electrochemical energy storage systems.[13] Numerical evaluation of the approach curve data furthermore provide kinetic constants that can be found for substrate characterization of various redox molecules[14] as well as for other important electrocatalytic reactions, i.e. the oxygen reduction reaction.[15]

In this work, SECM is used to analyze the VO^{2+}/VO_2^+ reaction in extension of our previous work[16], allowing for a quantitative comparison of various oxidized carbon materials towards the VO^{2+} to VO_2^+ oxidation.[9] In particular, the reduction reaction is analyzed by fitting the approach curve data of a feedback experiment at various substrate potentials,

[a] Dr. M. Steimecke, J. Carthäuser, E. Dieterich, Prof. Dr. M. Bron
Institut für Chemie, Technische Chemie I
Martin-Luther-Universität Halle-Wittenberg
Von-Danckelmann-Platz 4, 06120 Halle, Germany
E-mail: matthias.steimecke@chemie.uni-halle.de

[b] L. Fiedler
Present Address: Forschungszentrum Jülich GmbH, Helmholtz Institute Erlangen-Nürnberg for Renewable Energy (IEK-11), Cauerstr. 1, 91058 Erlangen, Germany
and
Department of Chemical and Biological Engineering, Friedrich-Alexander-Universität Erlangen-Nürnberg, Egerlandstr. 3, 91058 Erlangen, Germany

Supporting information for this article is available on the WWW under https://doi.org/10.1002/celc.202400158

which finally results in electron transfer constants of the reaction for substrates with different surface compositions. In the second part, a combined *in situ*-Raman-SECM[17] experiment is performed at a single graphene layer to analyze the contributions of basal and edge sites for the reaction. Site-specific quantification of kinetics and structure by a combined Raman-SECM approach characterizing multi-layered graphene has proven to be particularly suitable.[18]

Experimental Section

Synthesis and Chemicals

The materials used as substrates in this study were glassy carbon plates (GC, Sigradur G, HTW Hochtemperatur-Werkstoffe GmbH, Thierhaupten), graphite foil (Gfoil, GF-175, Graphite materials GmbH) as well as graphene. The GC plate was polished with 1 μm and 0.3 μm alumina suspension on a polishing cloth and then cleaned with water and ethanol prior to use. Graphite foil (Gfoil, GF-175, Graphite materials GmbH) was used as received. Oxidized samples were prepared by storing a piece of Gfoil or a GC sample without agitation in concentrated nitric acid (65 %, 14.4 mol L^{-1}, Carl Roth) for 2 and 7 days, respectively. Surface composition of all samples was analyzed by X-ray photoelectron spectroscopy (Omicron UHV system with a hemispherical EA125X electron energy analyzer with a five channeltron detector and DAR 400 X-Ray source with Al Kα radiation); the pass energy was 100 eV for survey spectra and 30 eV for spectra of the C1s and O1s binding energy regions. Electron micrographs of all samples were recorded with a Philips XL30 ESEM FEG scanning electron microscope (SEM, 10 keV) at different magnifications. Graphene was synthesized by ambient pressure-chemical vapor deposition (AP-CVD) onto an electro-polished copper substrate. Additional details can be found in a previous work.[19] A polymer-free transfer protocol was chosen to transfer graphene onto the conductive side of an indium-doped tin oxide electrode (ITO, 20 Ω per square, pgo GmbH, Iserlohn). For this purpose, the copper foil with graphene on top was placed in an aqueous 10 % ammonium peroxydisulfate (> 98 %, ACS, Carl Roth) solution. After ~3 h the copper was dissolved and the cleaned (acetone, water) ITO glass was used to carefully collect the remaining graphene film, which was then transferred into a bath of deionized water and collected again. Afterwards, the graphene@ITO film electrode was dried at 130 °C for 4 h in air.

SECM and Raman-SECM Setup

Glassy carbon, graphite foil and the respective oxidized samples were investigated towards their catalytic activity for vanadium redox reactions using approach curves in a commercial SECM setup (Sensolytics GmbH, Bochum) with a bi-potentiostat (PGSTAT128 N, Metrohm) using a commercial 10 μm platinum ultramicroelectrode (UME, $R_G = 30.7$, Sensolytics GmbH, Bochum) as working, a Ag | AgCl | $KCl_{sat.}$ (Meinsberger Elektroden) as reference and a piece of graphite foil as counter electrode. The substrate served as the second working electrode. All electrochemical experiments were performed in aqueous 10 mM $VOSO_4$ in 500 mM sulfate buffer (pH = 1.9, 1:1 mixture of 250 mM $KHSO_4$ and K_2SO_4 (both Carl Roth), respectively) purged with argon (99.999 %, Air Liquide). Before the experiments, the concentration of vanadyl ions was monitored by potentiometric titration using an automated titrator (877, Titrino plus, Metrohm) with commercial 0.1 M cer(IV) sulfate solution (Carl Roth). To obtain a constant response at the ultra-microelectrode, a pulse profile was applied consisting of 1 s at −0.2 V and 1.5 s at 1.3 V vs. the reference electrode (pulse profile 1). An in-depth discussion of the advantages and necessity of a pulse profile is presented in the results part. Prior to performing an approach curve, the pulse profile was applied 50 to 75 times to obtain a constant current response. The microelectrode was then lowered with 5 μm $step^{-1}$ to the substrate until touching the surface, while the pulse profile was constantly applied. This procedure was repeated for several substrate potentials between −0.1 and 0.6 V. Single experiments were also additionally carried out at −0.2 and 1.0 V. Individual approach curves were recorded at two to four different locations of the samples. For data evaluation, the mean current value of the last 500 ms of the oxidizing pulse (1.3 V) was calculated and related to the current at an infinite distance (~200 μm). In an additional experiment, each substrate was used as primary working electrode and cyclic voltammograms between −0.2 V and 1.4 V were performed with a scan rate of 50 mV s^{-1} in the very same setup. The exposed area of the substrates was about 3.1 cm^2.

In case of graphene, a needle-type ultramicroelectrode was fabricated following a procedure presented by the Schuhmann group.[20] Briefly, a piece of platinum wire (25 μm diameter, Goodfellow) was placed in the middle of a quartz glass capillary (QSIL ilmasil PN, O.D. = 0.9 ± 0.05 mm, I.D. = 0.3 ± 0.1 mm) and fixed in a laser-assisted micropipette puller system (Sutter P-2000). A clamp blocked the pulling mechanics of the instrument and the quartz glass around the Pt wire was heated (relevant parameters of the laser puller: HEAT = 630, FIL = 5) while both capillary ends were connected to a vacuum pump. This procedure was repeated until the Pt wire was fixed in the molten quartz capillary. Afterwards, pulling was initiated applying the following parameters: HEAT = 630, FIL = 2, VEL = 90, DEL = 100, PUL = 220. The pulled Pt wire in quartz glass was contacted to a copper wire using solder (both ~200 μm diameter) from the open end of the capillary employing a commercial heat gun. Ultramicroelectrodes were optically inspected, cut, if necessary, polished with a home-built polishing instrument on 0.3 μm alumina polishing paper (Sensolytics GmbH, Bochum) and cleaned in acetone (99.5 %, Carl Roth) and water in an ultrasonification bath (Sonocool, Bandelin). All handling steps with the needle-type ultramicroelectrode were carried out with ESD-saved equipment to avoid damage by electrostatic discharge.[21] Initial electrochemical characterization was then performed in 5 mM $[Ru(NH_3)_6]Cl_3$ (98 %, Acros Chemicals) in 100 mM KCl (99.5 %, Carl Roth) between −0.4 and 0.1 V with 10 mV s^{-1}.

To characterize the graphene layer on ITO *in situ*, a home-built SECM instrument[17] consisting of a z-stepper motor (Sensolytics GmbH) and an inverted Raman microscope system (Renishaw) with x-y stage, 532 nm laser, a grating of 1800 l mm^{-1} and a CCD camera was used. Again, the substrate served as second working electrode and was analyzed by Raman microscopy from the backside of the transparent electrode material during the experiment. In contrast to the setup described before, a Pt wire served as counter electrode, the concentration of vanadyl sulfate was increased to 50 mM and the pulse profile was modified as follows: 2 s at −0.2 V and 2 s at 1.4 V (pulse profile 2). The needle-type ultramicroelectrode ($R_G = 45.9$) was lowered to touch a bare region of the ITO under optical control and lifted up for 2 μm. Line scans with step width of 500 nm starting from the bare ITO region to the single layer graphene crystal were performed and the pulse profile as well as a Raman spectrum from 100–3200 cm^{-1} were recorded in parallel at every position. This combined experiment was performed at the very same line with three substrate potentials (0.8 V, 0.3 V and −0.2 V). All experiments were carried out at room temperature and under continuous argon saturation.

Results and Discussion

Figure 1a shows a schematic representation of the feedback mode of SECM, which is able to provide kinetic data of an electrochemical reaction at the substrate electrode (in this case carbon materials) by analyzing approach curve data. This technique requires a constant current response of the microelectrode (Figure 1c, red curve). This is usually obtained by applying a constant potential in the diffusion limited current region. In this case, however, a constant potential in the VO^{2+} oxidation region (1.3 V) leads to a constant decrease of the current at the UME (Figure 1c, black curve), probably due to electrode fouling or product precipitation. In contrast, a constant UME response (Figure 1b, red curve) was obtained by using a pulsed chrono-amperometric profile. The respective potentials were derived from initially recorded cyclic voltammograms in 0.5 M sulfate buffer solution (pH = 2) with and without the addition of 10 mM $VOSO_4$ (Figure 1b). CV data was in accordance with our reported results.[16]

The final procedure consist of a regeneration pulse of 1 s at −0.2 V (E_1), which is close to the hydrogen adsorption region (H_{upd}) at platinum, in order to reduce various VO_x surface species[22], which might have formed and are blocking the surface, and a detection pulse of 1.5 s at 1.3 V (E_2), where the reaction of interest, i.e. oxidation of VO^{2+} to VO_2^+, is monitored at the UME (Figure 1d). For evaluation, a mean current value is calculated from the last 500 ms of the oxidative pulse. Additionally, the current response of the pulse profile shows a quantitative correlation between the VO^{2+} concentration and the oxidation current from 0 to 10 mM $VOSO_4$ (inset in Figure 1d). This correlation is of particular importance because a decrease of UME current resulting from the depletion of VO^{2+} ions during approach curve experiments and slow reduction kinetics[23] of the substrate have to be expected, which would hinder a strong positive feedback. Two prominent carbon materials were used as flat model electrodes for the determination of kinetic data by approach curve experiments, namely glassy carbon (GC) and graphite foil (Gfoil). Furthermore, surface modified derivates of the samples (GC_ox, Gfoil_ox) were obtained by storing the samples in concentrated nitric acid for several days at room temperature. This method was chosen to avoid any mechanical treatment of the samples, which occurs during heating and mixing and which may affect the final porosity of the samples. The intactness of the surface microstructure was confirmed by scanning electron microscopy (Figure S1 in the SI). Furthermore, surface elemental composition was analyzed by X-ray photoelectron spectroscopy. The results differ between the individual carbon materials (Figure 2a and SI Figure S2). The initial oxygen content of GC was found to be 8.9 at.% and increased to 11.7 at.% after 7 days of acid

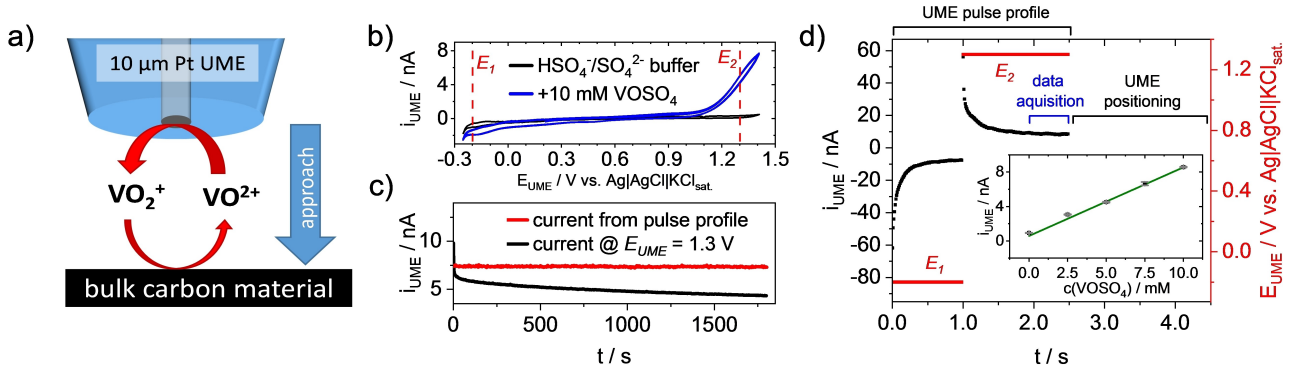

Figure 1. a) Schematic representation of the SECM setup capable of providing kinetic information about the substrate electrode by performing approach curves, b) cyclic voltammograms at 50 mV s^{-1} of a 10 µm Pt microelectrode in Ar-saturated sulfate buffer solution (pH = 2) with and without the addition of $VOSO_4$, c) current response of a pulsed potential profile (red) in comparison to a constant potential (black, E = 1.3 V) and d) the current response of a single pulse profile with an inset of the mean current and standard deviation of ten consecutive pulses in dependence of different $VOSO_4$ concentration from 0–10 mM in the solution. The slope of the regression (green) could be determined as 0.757 nA mM^{-1} (R^2 = 0.997).

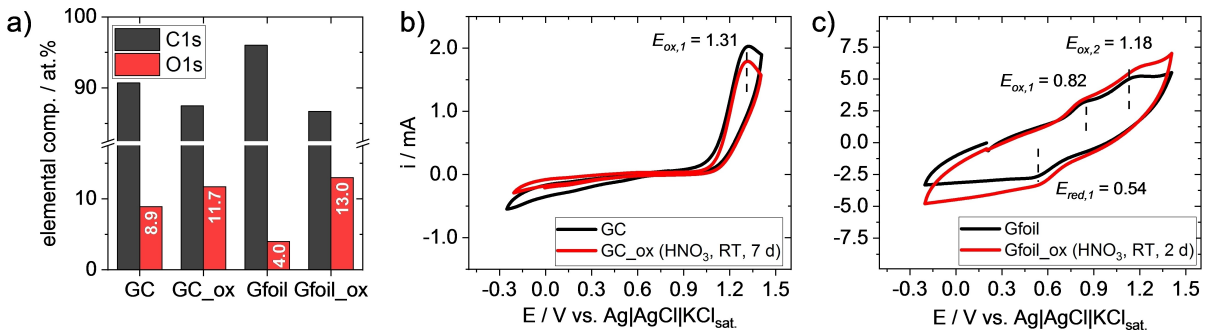

Figure 2. a) Surface composition derived from X-ray photoelectron spectra of the C1s and O1s region of all samples (see supplementary information for more details) and cyclic voltammograms of b) both glassy carbon and c) both graphite foil samples at 50 mV s^{-1} in 10 mM $VOSO_4$ in 0.5 M sulfate buffer solution, the title of the ordinate in c) is the same as in b).

treatment. An initially high oxygen content was also reported by others for GC[24] and in particular for the GC (HTW, Sigradur G®)[25] used in this work. As a result, nitric acid treatment has only little impact on the surface composition of the GC due to the initially high oxygen content. In contrast, surface oxygen content of the graphite foil increased from 4.0 to 13.0 at.% after 2 days of acid treatment. As the structure was still intact after treatment, the oxygen containing functional groups may be present primarily at the edges of the graphite crystals. However, the C1s detail scan also showed decreased sp2 carbon presence after treatment (compare Figure S2e and g in the SI). Electrochemical characterization of the substrates was performed in the very same electrolyte as used for the initially described SECM feedback method and the results are compared in Figure 2b and c. In case of GC (Figure 2b), a dominant peak attributed to oxidation of VO^{2+} can be found at 1.31 V, whereas the reduction process is spread over a broad potential region without a clear peak formation. For graphite foil (Figure 2c), the oxidation of VO^{2+} is separated into two distinct peaks at 0.82 V and 1.18 V resulting from individual edge and basal plane contribution.[12] A broad reduction region can also be found at this sample, however, a peak is also formed at 0.54 V. In both cases, the influence of oxidative treatment (7 or 2 days in 14.4 M HNO_3, respectively) appears to be negligible both in peak position and in height, in this case.

All characterized samples were used as substrate electrodes for SECM feedback experiments and individual approach curves (schematically displayed in Figure 1a) were performed for each sample at two to four different locations at substrate potentials of −0.1 V to 0.6 V. Data analysis was following a procedure suggested by Liu and Bard for the determination of the kinetics of the oxygen reduction reaction (ORR) on platinum substrate.[15]

A fully evaluated data set including the fits and equations for untreated glassy carbon can be found in Figure S3 and in the text of the SI. Selected data sets and fits are also shown in Figure 3a including the two limiting cases of positive (black curve) and negative feedback (blue curve) calculated according to the equations summarized by Lefrou and Cornut.[26] All approach curve data of the selected potentials can be found in between both cases. At $E_{sub.} = -0.2$ V a positive feedback can be observed at larger distances, turning into a negative feedback closer to the electrode, whereas at −0.1 V and 0.6 V the current is corresponding to a negative feedback. For a better illustration of all substrate potential steps applied, the data is shown in a logarithmic plot of the normalized distance in Figure 3b. Additionally, a substrate potential more positive than the equilibrium potential of the reaction was applied (1.0 V). In this case, the fitting process (Figure 3a, grey squares) can no longer reproduce the recorded data due to the transition of a feedback into a competitive SECM experiment. From the evaluation of the fitted data (see equations 1 to 8 and text in the SI), potential dependent rate constants k are calculated and lg(k) is plotted against the overpotential η of the reaction (Figure 3c) in form of a TAFEL plot. The equilibrium potential was calculated from the standard redox potential E_0 of the VO^{2+}/VO_2^+ reaction corrected by the pH shift and the used reference electrode. Finally, electron transfer constants k_0 ($\eta = 0$) and TAFEL slopes can be determined. Table 1 summarizes the range of the obtained electron transfer constants and TAFEL slops from linearization for the bare and oxidized substrates. The corresponding TAFEL plots are displayed in Figure S4. In case of glassy carbon (GC), a k_0 twice as high for the oxidized compared to the untreated sample can be found. Additionally, the TAFEL slope is slightly decreased but still high in comparison to various other redox reactions. However, the oxygen content of the untreated GC was already high and showed a small increases from 8.7 to 11.7 at.% due to acid treatment. In case of graphite foil (Gfoil), the values of the oxidized sample are in the same range of the untreated samples although the oxygen content strongly increases from 4.0 to 13.0 at.%. Focusing on

Table 1. Electron transfer constants and Tafel slops derived from Tafel plots (see Figure S4 in the SI).

sample	$k_0/10^{-4}$ cm s^{-1}	TAFEL slope/mV dec^{-1}
GC	0.7–2.4	955–1217
GC_ox	2.5–5.9	428–903
Gfoil	1.4–7.7	633–1525
Gfoil_ox	3.2–4.1	726–1351

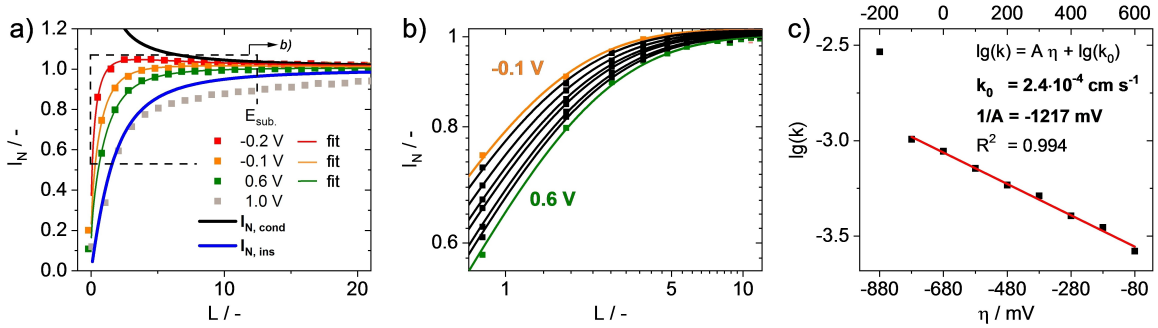

Figure 3. a) Selected approach curves: normalized UME currents in dependence of the normalized distance L (see equation 1 in the SI) with measured data (full squares) and fitted curves (lines); $I_{N, cond}$ and $I_{N, ins}$ are calculated according to the equations of Lefrou and Cornut,[26] b) logarithmic plot of selected approach curves from (a) with fit and c) TAFEL plot: potential dependent rate constants k derived from approach curve fits in dependence of the overpotential η, all for the untreated glassy carbon substrate.

the electron transfer constants, the results are within the reported values from cyclic voltammetry. For glassy carbon Wu et al.[27] found $0.54 \cdot 10^{-4}$ cm s^{-1} whereas Sum et al.[28] reported $7.5 \cdot 10^{-4}$ cm s^{-1}. Yamamura et al.[10] reported $1.3 \cdot 10^{-4}$ cm s^{-1} for pyrolytic graphite with exposed basal plane (c-PG) which is comparable to the material used here. However, an in-depth discussion is hardly possible because most of them do not include information about the GC or graphite surface composition. It is important to note that the sample porosity remains unaffected after oxidative treatment in our case. Higher porosity can increase the apparent kinetic constant by several orders of magnitude[7] which is not the case here and allows for a straightforward comparison of untreated and oxidized sample. For the sake of completeness, Table 1 also displays the Tafel slops where in all cases the values are extraordinary high, however, unusually high Tafel slopes of the VO_2^+ reduction were also reported by others.[11]

To gain additional insight into structural features of carbon samples, which might be responsible for high activity in vanadium redox reactions, the presented pulse profile was also used to locally resolve the activity towards the VO^{2+}/VO_2^+ redox couple of a single layer graphene crystal. For this purpose the combined Raman SECM instrumentation[17] is perfectly suitable to verify the location and structure of the used single layered graphene. Furthermore, the activity of edge sites of the graphene crystal is of particular interest in comparison to the basal plane regions. For increased position resolution, a smaller UME was used which was fabricated by a laser puller-assisted method as described in the experimental part. This UME was characterized before operation and all details can be found in Figure S5. The diameter of the Pt metal was determined to be 2.7 µm by cyclic voltammetry and optical microscopy. For the *in situ*-experiments, the VO^{2+} concentration was increased to 50 mM and the pulse durations were slightly extended (see experimental part). Graphene as substrate electrode was synthesized onto copper foil by AP-CVD method and transferred by a polymer-free method to the ITO glass electrode. The transfer process avoids polymer contamination; however, the graphene film easily cracks into small pieces that partially delaminate after contact with the solution. Graphene delamination can be carried out by electrochemical procedures and can be attributed to ion intercalation effects.[29] On the other hand, delamination might be a result of the etching of the ITO electrode under the prevailing pH condition.[30] Thus, it was a challenge to maintain a stable film over the whole experiment. Since we only found very small graphene crystals after the transfer, we decided not to carry out kinetic investigations by approach curves for this substrate, although this has already been successfully demonstrated for other mediators on large graphene crystals.[31]

Figure 4a visualizes the experimental setup. An UME with smaller diameter was used for the combined experiment to reflect the size of the Raman laser spot (~1 µm). The sample was positioned and moved in such a way that the transition region from bare ITO to graphene was always investigated. Meanwhile, three different potentials were sequentially applied to the substrate and both the pulse profile as well as the Raman spectra acquisition were conducted in parallel at each position. Based on the results presented above, substrate potentials were chosen as 0.8 V (~110 mV above the equilibrium potential), 0.3 V (medium overpotential) and −0.2 V (high overpotential of the reduction) and the electrochemical results can be found in the upper part of Figure 4b. Data of the evaluated Raman spectra, here 2D band intensity as the most intensive band, are displayed in the lower part. At 0.8 V, the UME current from the pulse profile continuously decreases until a minimum between a relative position of 15–18 µm is reached. Afterwards, the current increases again to its initial value. Raman data suggests the presence of a small graphene crystal between 15–18 µm followed by a larger crystal starting from 20 µm. As this region shows the lowest UME current, a depletion of VO^{2+} ions by consumption at the substrate can be assumed. A competitive

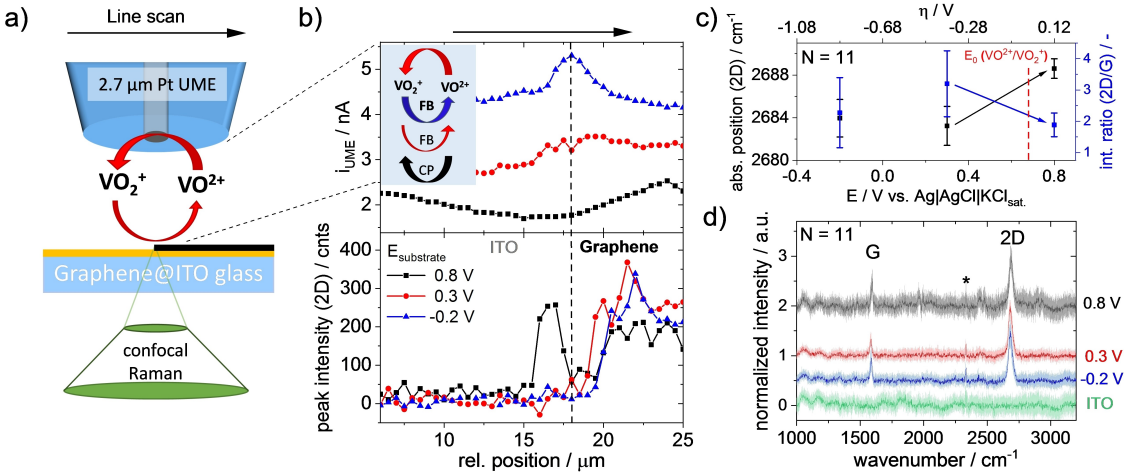

Figure 4. a) Scheme (not true to scale) of a 2.7 µm Pt microelectrode over a graphene thin film on an ITO electrode; Raman probing was realized from the backside of the transparent electrode, b) top: UME response from the pulsed profile of the edge region with an inset of data interpretation for the scheme (FB – feedback mode, CP – competitive mode) and bottom: the evaluation of the 2D band intensity recorded in parallel at the same position, c) evaluation of the potential dependent 2D band position and the 2D/G ratio of the *in situ*-Raman data and d) averaged spectra with standard deviation of the graphene-covered region used for evaluation in (b and c), the asterix marks the signal of N_2 from air.

process resulting from the slightly oxidative potential at the substrate takes place, in accordance with the position of the oxidation peak observed in the CV of the graphite samples in Figure 2c ($E_{ox,1} = 0.82$ V). Since the current increases again after crossing this region towards the basal plane graphene, crystal edges may serve as active centers at this potential. To force a feedback configuration as demonstrated in the approach curve experiments before, two potentials at medium (0.3 V) and high overpotential (−0.2 V) of the VO_2^+ reduction where applied. The average UME current increases from ~2 nA to ~3 and ~4.5 nA, respectively, indicating an increased feedback. In case of −0.2 V a distinct peak of a strong positive feedback between 17 and 20 μm is observed, which is markedly less pronounced at a medium overpotential (0.3 V). Raman data evaluation of the 2D band intensity indicates loss of the small graphene crystal between 15 and 18 μm possibly by detaching. The remaining large crystal shows increased positive feedback (~700 pA) at the edge region in comparison to the basal planes of graphene and the bare ITO substrate. Beside the 2D band intensity, the 2D band position as well as 2D/G ratio were analyzed from the full spectra (Figure 4c). The averaged spectra including standard deviation of the large graphene crystal region (20–25 μm) with the relevant bands are shown in Figure 4d. Beside the high 2D/G ratio at −0.2 and 0.3 V the absence of the D band in the spectra points to a defect free graphene crystal. At higher oxidative potential (0.8 V), the 2D band position increases from 2683 to 2689 cm^{-1} and 2D/G ratio decreases to <2. Both observations are described for polarized graphene samples during *in situ* electrochemical experiments[32] confirming again that the large crystal is attached to the ITO surface and polarized during the experiments. For the sake of completeness, it should be mentioned that the maximum feedback at −0.2 V was found at a position without any Raman signal of graphene. This observation can be explained by the detaching of the edge and protruding into the solution, which results an offset between electrochemical and spectroscopic response. Graphitic structures with exposed edges were also confirmed by SECCM technique.[33] In conclusion, it was found out that the edges of a graphene crystal showed increased activity for both the oxidation of VO^{2+} at relatively low overpotential and for the reduction of VO_2^+ at very high overpotentials in comparison to the basal planes.

Conclusions

In this work, carbon model substrates were analyzed towards kinetic data as well as relevant structural features for the VO^{2+}/VO_2^+ redox reaction, which is of relevance for vanadium redox flow batteries. An SECM procedure with a pulsed potential at the microelectrode was presented, allowing for a constant electrochemical response of the UME in VO^{2+} containing sulfate buffer solution, which is not achieved in potentiostatic experiments. This approach was then used to determine the reaction kinetics over bare and oxidized carbon samples in an SECM feedback experiment. Electron transfer coefficients k_0 of glassy carbon and graphite substrates and their oxidized derivates were calculated from data evaluation of the approach curve fitting and values ($0.7–7.7 \cdot 10^{-4}$ cm s^{-1}) comparable to those obtained from cyclic voltammetry were found. For the oxidized samples the results seems to depend on the material. In case of oxidized GC, a slight improvement might be concluded since the electron transfer constant doubles, albeit with a significant error, whereas in case of graphite k_0 is not affect although the oxygen content increases from 4.0 to 13.0 at.%.

Furthermore, a Raman-coupled SECM experiments at graphene crystals deposited onto ITO identified edge sites as active parts for the VO_2^+ reduction during feedback experiment (at rather high overpotentials) and for the VO^{2+} oxidation in a competitive approach at a moderate overpotential. In both cases, the edge region showed increased activity in comparison to basal planes of the graphene.

Supporting Information

The authors have cited additional references within the Supporting Information.[26],[34]

Acknowledgements

The authors are thankful to Annett Quetschke and Eik Koslowski from our institute for SEM for XPS measurements. We would further like to thank Dr. Thomas Erichsen and Dr. Michaela Nebel from Sensolytics GmbH, Bochum, for discussion and support. Open Access funding enabled and organized by Projekt DEAL.

Conflict of Interests

The authors declare no conflict of interest.

Data Availability Statement

The data that support the findings of this study are available from the corresponding author upon reasonable request.

Keywords: scanning electrochemical microscopy · Raman microscopy · vanadium redox flow battery · graphene · carbon materials

[1] M. Skyllas-Kazacos, M. Rychcik, R. G. Robins, A. G. Fane, M. A. Green, *J. Electrochem. Soc.* **1986**, *133*, 1057.
[2] A. W. Bayeh, D. M. Kabtamu, Y.-C. Chang, T. H. Wondimu, H.-C. Huang, C.-H. Wang, *Sustain. Energy Fuels* **2021**, *5*, 1668.
[3] D. J. Suárez, Z. González, C. Blanco, M. Granda, R. Menéndez, R. Santamaría, *ChemSusChem* **2014**, *7*, 914.
[4] A. Bourke, D. Oboroceanu, N. Quill, C. Lenihan, M. A. Safi, M. A. Miller, R. F. Savinell, J. S. Wainright, V. SasikumarSP, M. Rybalchenko, et al., *J. Electrochem. Soc.* **2023**, *170*, 30504.
[5] B. Sun, M. Skyllas-Kazacos, *Electrochim. Acta* **1992**, *37*, 1253.
[6] H. Radinger, *ChemPhysChem* **2021**, *22*, 2498.
[7] J. Friedl, U. Stimming, *Electrochim. Acta* **2017**, *227*, 235.

[8] M.-A. Goulet, M. Skyllas-Kazacos, E. Kjeang, *Carbon* **2016**, *101*, 390.
[9] M. Steimecke, S. Rümmler, N.-F. Schuhmacher, T. Lindenberg, M. Hartmann, M. Bron, *Electroanalysis* **2017**, *29*, 1056.
[10] T. Yamamura, N. Watanabe, T. Yano, Y. Shiokawa, *J. Electrochem. Soc.* **2005**, *152*, A830.
[11] M. Gattrell, J. Park, B. MacDougall, J. Apte, S. McCarthy, C. W. Wu, *J. Electrochem. Soc.* **2004**, *151*, A123–A130.
[12] N. Pour, D. G. Kwabi, T. Carney, R. M. Darling, M. L. Perry, Y. Shao-Horn, *J. Phys. Chem. C* **2015**, *119*, 5311.
[13] M. Steimecke, *Encyclopedia* **2023**, *3*, 1320.
[14] A. K. Neufeld, A. P. O'Mullane, *J. Solid State Electrochem.* **2006**, *10*, 808.
[15] B. Liu, A. J. Bard, *J. Phys. Chem. B* **2002**, *106*, 12801.
[16] M. Steimecke, S. Rümmler, M. Kühhirt, M. Bron, *ChemElectroChem* **2016**, *3*, 318.
[17] M. Steimecke, G. Seiffarth, M. Bron, *Anal. Chem.* **2017**, *89*, 10679.
[18] N. B. Schorr, A. G. Jiang, J. Rodríguez-López, *Anal. Chem.* **2018**.
[19] X. Lu, X. Yang, M. Tariq, F. Li, M. Steimecke, J. Li, A. Varga, M. Bron, B. Abel, *J. Mater. Chem. A* **2020**, *8*, 2445.
[20] B. B. Katemann, W. Schuhmann, *Electroanalysis* **2002**, *14*, 22.
[21] N. Nioradze, R. Chen, J. Kim, M. Shen, P. Santhosh, S. Amemiya, *Anal. Chem.* **2013**, *85*, 6198.
[22] W. Wang, X. Fan, Y. Qin, J. Liu, C. Yan, C. Zeng, *Electrochim. Acta* **2018**, *283*, 1313.
[23] M. Gattrell, J. Qian, C. Stewart, P. Graham, B. MacDougall, *Electrochim. Acta* **2005**, *51*, 395.
[24] P. Chen, M. A. Fryling, R. L. McCreery, *Anal. Chem.* **1995**, *67*, 3115.
[25] Y. Yi, G. Weinberg, M. Prenzel, M. Greiner, S. Heumann, S. Becker, R. Schlögl, *Catal. Today* **2017**, *295*, 32.
[26] C. Lefrou, R. Cornut, *ChemPhysChem* **2010**, *11*, 547.
[27] X. W. Wu, T. Yamamura, S. Ohta, Q. X. Zhang, F. C. Lv, C. M. Liu, K. Shirasaki, I. Satoh, T. Shikama, D. Lu et al, *J. Appl. Electrochem.* **2011**, *41*, 1183.
[28] E. Sum, M. Rychcik, M. Skyllas-Kazacos, *J. Power Sources* **1985**, *16*, 85.
[29] K. Verguts, J. Coroa, C. Huyghebaert, S. de Gendt, S. Brems, *Nanoscale* **2018**, *10*, 5515.
[30] M. Senthilkumar, J. Mathiyarasu, J. Joseph, K. L. N. Phani, V. Yegnaraman, *Mater. Chem. Phys.* **2008**, *108*, 403.
[31] a) N. L. Ritzert, J. Rodríguez-López, C. Tan, H. D. Abruña, *Langmuir* **2013**, *29*, 1683; b) R. Chen, N. Nioradze, P. Santhosh, Z. Li, S. P. Surwade, G. J. Shenoy, D. G. Parobek, M. A. Kim, H. Liu, S. Amemiya, *Angew. Chem. Int. Ed.* **2015**, *54*, 15134.
[32] M. Kalbac, A. Reina-Cecco, H. Farhat, J. Kong, L. Kavan, M. S. Dresselhaus, *ACS Nano* **2010**, *4*, 6055.
[33] A. G. Guell, A. S. Cuharuc, Y.-R. Kim, G. Zhang, S. Tan, N. Ebejer, P. R. Unwin, *ACS Nano* **2015**, *9*, 3558.
[34] a) J. Lawton, S. Tiano, D. Donnelly, S. Flanagan, T. Arruda, *Batteries* **2018**, *4*, 40; b) F. Marken, J. C. Eklund, R. G. Compton, *J. Electroanal. Chem.* **1995**, *395*, 335.

Manuscript received: February 16, 2024
Revised manuscript received: March 22, 2024
Version of record online: April 25, 2024